

# Specific heat and its high-order moments in relativistic heavy-ion collisions from a multiphase transport model

Ru-Xin Cao(曹汝鑫)

*Shanghai Institute of Applied Physics, Chinese Academy of Sciences, Shanghai 201800, China*

*Key Laboratory of Nuclear Physics and Ion-beam Application (MOE),*

*Institute of Modern Physics, Fudan University, Shanghai 200433, China and*

*School of Nuclear Sciences and Technology, University of Chinese Academy of Sciences, Beijing 100049, China*

Song Zhang(张松)\* and Yu-Gang Ma(马余刚)†

*Key Laboratory of Nuclear Physics and Ion-beam Application (MOE),*

*Institute of Modern Physics, Fudan University, Shanghai 200433, China and*

*Shanghai Research Center for Theoretical Nuclear Physics, NSFC and Fudan University, Shanghai 200438, China*

We studied the energy dependence of specific heat extracted from the fluctuation of temperature fitted by the  $p_T$  spectra at  $\sqrt{s_{NN}} = 7.7$  GeV to 200 GeV in Au + Au collisions by using AMPT model. The results were compared with those from other models and some difference at low  $\sqrt{s_{NN}}$  was found. To explain the difference and describe the properties of the hot matter at low  $\sqrt{s_{NN}}$ , we derived new quantities  $C_v^\xi$  and  $C_v^{\xi*}$  for describing specific heat in heavy-ion collisions. We found that the alternative method could describe thermal properties of the matter involving  $C_v^{\xi*}$  together with its high order moments, namely skewness and kurtosis, extracted from the event-by-event distribution of  $C_v^{\xi*}$ . The proposed observables could shed light on the QCD phase transition along with critical point in heavy-ion collisions.

## I. INTRODUCTION

During the past few decades, amount efforts have been made on researching the hot dense quark matter created in relativistic heavy-ion collisions. Plenty of evidences for proving the existence of quark-gluon plasma (QGP) were found in relativistic heavy-ion collisions and aroused the interests to explore the properties of the hot dense matter created under the extreme conditions [1–6]. Specific heat was carried out as one of the signals of phase transition in partonic level as well as nucleonic level and helps to inspect thermal properties of nuclear matter. In partonic level, the Lattice QCD predicted the phase transition as a crossover at zero baryon-chemical potential ( $\mu_B = 0$ ) but while a first order phase transition could occur at finite baryonic density  $T_c$  [7–13]. In nucleonic level, a liquid gas phase transition can occur at sub-saturation density and finite temperature [14–24]. Physicists paid more attention to the temperature fluctuation with specific heat.

According to phase transition theory, the long-range correlation diverges rapidly when a thermodynamic system evolves close to critical point, meaning the quarks and gluons, rather than mesons and baryons define the relevant degrees of freedom of the matter created in the collisions. As a response to the system perturbation the specific heat will diverge when the system evolves close to the critical point. In statistical physics the heat capacity can be associated with the fluctuation of temperature. Some researches suggested to extract heat capacity

from the event-by-event distribution of ensemble temperature [7–12, 20, 22, 25–30]. For near the critical point, the specific heat  $C_V$  can be expressed as a function in terms of a power law,  $C_V \propto |T - T_c|^{-\alpha}$ , here  $T_c$  is the critical temperature and  $\alpha$  the critical exponent.

In this study, a multiphase transport (AMPT) model [31–33] was adopted to simulate Au + Au collisions at  $\sqrt{s_{NN}} = 7.7, 11.5, 14.5, 19.6, 27, 39, 62.4,$  and 200 GeV. Energy dependence of  $C_V$  was obtained by the above introduced method and compared with results extracted through the same temperature fluctuation method by the Hadron Matter (HM) [28], Hadron Matter via Quark Gluon Matter [28], Quark Gluon Matter (QGM) [28], Hadron Resonance Gas (HRG) models as well as data of the STAR Collaboration [29, 34]. However, it was found the specific heat obtained from the AMPT showed obvious depression at low  $\sqrt{s_{NN}}$ , similar to some other models [28, 29, 34]. The insensitivity of temperature fluctuation in the AMPT drove our study to try another derivation of heat capacity from the basic definition of heat capacity based on some assumptions. The derivation in this study gives an effective specific heat  $C_v^{\xi*}$  which is expressed by the characteristic event ( $\xi$ )’s kinetic quantities, and plots the event-by-event distribution to obtain the skewness and kurtosis to describe the statistical properties of  $C_v^{\xi*}$ . The new derived  $C_v^{\xi*}$  together its with skewness and kurtosis give insight of the evolution of thermodynamical properties of the emitted particles and describe energy dependence of specific heat, which could be performed in experiments.

The paper is organized as follows: in Sec. II, a brief introduction was given to a multiphase transport (AMPT) model and the results on the energy dependence of specific heat obtained from the event-by-event fluctuation

\* Email: song\_zhang@fudan.edu.cn

† Email: mayugang@fudan.edu.cn

in Au + Au collisions simulated by AMPT were demonstrated, then the extracted results were compared with those from other models and the STAR Collaboration, which pointed out the difference and the uncertainty at low  $\sqrt{s_{NN}}$  in the AMPT frame. In Sec. III, a brief qualitative explanation for the difference was given and the study started from the definition of specific heat to derive the formula expressed by kinetic quantities called  $C_v^{\xi^*}$ . After which in Sec. IV, the results for mean value, skewness, kurtosis of event-by-event distributions for  $C_v^{\xi^*}$  were shown with explanation of the meaning of those moments, which gave insight of emitted particles' thermodynamic properties. Finally, the last part presented a brief summary on our work in Sec. V.

## II. AMPT RESULTS AND COMPARISON

### A. Introduction to AMPT

A multiphase transport (AMPT) model [31–33] composed of four parts to simulate the relativistic heavy-ion collisions. It has successfully described various phenomena of heavy-ion collisions at the RHIC and LHC energies and becomes a well-known event generator. The AMPT has two versions: String Melting (SM) and Default. In SM version, Heavy Ion Jet Interaction Generator (HIJING) [35, 36] is used to simulate the initial conditions, then Zhang's Parton Cascade (ZPC) [37] is used to describe interactions for partons which are from all of hadrons in the HIJING but spectators, after which a simple Quark Coalescence Model is used to describe hadronization process, finally A Relativistic Transport (ART) model [38] is used to simulate hadron rescattering. The Default version AMPT only conducts the minijet partons in partonic scatterings via ZPC and used the Lund string fragmentation to perform hadronization.

AMPT model [31, 33] has been widely used in describing the  $p_T$  spectrum, yield and energy dependence of particles such as pion, kaon,  $\phi$ , proton and  $\Omega$  produced in heavy-ion collisions [32, 39, 40] as well as extracting the flow or temperature during evolution etc [29, 41–43]. Chiral and magnetic related exotic phenomena can also be well described by the AMPT model [44–49]. More details and set for parameters can be found in [31–33]. Our present study used both versions to simulate Au + Au collisions at  $\sqrt{s_{NN}} = 7.7, 11.5, 14.5, 19.6, 27, 39, 62.4,$  and 200 GeV in the impact parameter range of 0–4.7 fm corresponding to centrality 0–10%.

### B. $C_V$ from fluctuation

Firstly, an event-by-event fluctuation method was used to study the center of mass energy  $\sqrt{s_{NN}}$  dependence of specific heat. As noted in Refs. [28, 29], since the low multiplicity caused relatively large error in fitting on  $p_T$  spectrum, we combined simulation data from a few events

to one linked event, thus we increased mean multiplicity in one event more than 1000, as other did in Ref. [29].

The effective temperature,  $T_{eff}$ , of a  $\pi^+$  system at final state is obtained via fitting  $p_T$  spectrum by using the exponential distribution [32, 50, 51]:

$$\frac{1}{p_T} \frac{dN}{dp_T} = A e^{\frac{-p_T}{T_{eff}}}. \quad (1)$$

$\pi^+$  system is chosen for the calculations with kinetic window,  $p_T < 2$  GeV/c and  $-1 < y < 1$ . The effective temperature,  $T_{eff}$ , actually stands for the slope of  $p_T$  spectrum and consists of two parts, i.e. the kinetic temperature  $T_{kin}$  and contribution from radial flow  $\langle\beta_T\rangle$  [29],

$$T_{eff} = T_{kin} + f(\langle\beta_T\rangle), \quad (2)$$

where the kinetic freeze-out temperature,  $T_{kin}$ , characterizes thermal motion of emitted particles, and  $f(\langle\beta_T\rangle)$  reflects transverse radial flow contribution. As we are discussing  $\pi^+$  system, the relation in Eq. (2) can be approximately written as [29],

$$T_{eff} \approx T_{kin} + m_0 \langle\beta_T\rangle^2, \quad (3)$$

where  $m_0$  is the mass of  $\pi^+$ .

For a system in equilibrium, its heat capacity is related to the fluctuation of event-by-event temperature distribution [7, 10, 11, 30],

$$P(T) \propto e^{-\frac{C}{2} \frac{(\Delta T)^2}{\langle T \rangle^2}}, \quad (4)$$

where  $\langle T \rangle$  is mean value of event-by-event distribution of temperature and  $\Delta T = T - \langle T \rangle$  is variance of temperature. And the expression can be further derived as [29]:

$$\frac{1}{C} = \frac{\langle T_{kin}^2 \rangle - \langle T_{kin} \rangle^2}{\langle T_{kin} \rangle^2} \approx \frac{\langle T_{eff}^2 \rangle - \langle T_{eff} \rangle^2}{\langle T_{kin} \rangle^2}. \quad (5)$$

When multiplicity  $N$  is taken into account, we can get specific heat per particle as the following

$$C_V = \frac{C}{N}. \quad (6)$$

In this section we choose  $T_{kin}$  to determine  $C_V$  since the variances of  $T_{kin}$  and  $T_{eff}$  are close enough to each other as mentioned in Ref. [29].

Figure 1 showed the  $p_T$  spectrum in linked events fitted by Eq. (1), then the effective temperature for every linked events was obtained as shown in Fig. 2(a). Meanwhile, in our present work we calculated transverse flow velocity  $\beta_T$  by  $\beta_T = \beta_r \cdot r_T$ , where  $\beta_r$  is the transverse velocity and  $r_T$  is the transverse coordinates of particles at kinetic freeze-out state, which is different from Refs. [29, 52] where a Blast-Wave Model was used to obtain a fit parameter also denoted by  $\beta_T$ . Two different definition and methods on  $\beta_T$  caused some difference for the event-by-event distribution, but as mentioned in Ref. [29], fluctuation in  $\beta_T$  could be dominant in small, asymmetric and

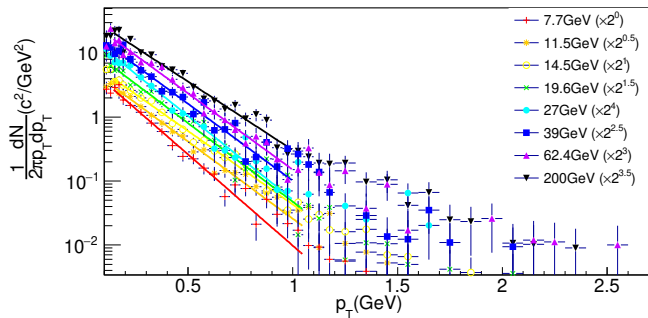


FIG. 1. The linked  $p_T$  spectrum with  $-1 < y < 1$  at  $\sqrt{s_{NN}} = 7.7 - 200$  GeV in 0–10% central Au + Au collisions by using the String Melting AMPT.

non-central collisions. However, our work focus on Au-Au system, the fluctuation from  $\beta_T$  could be negligible.

After removing transverse radial flow contribution by Eq. (3), the distribution of event-by-event  $T_{kin}$  is presented in Fig. 2(b) at the centrality of 0–10% and  $\sqrt{s_{NN}} = 7.7 - 200$  GeV. It is clearly seen that  $T_{kin}$  is much lower than  $T_{eff}$  because the transverse radial flow is taken off as much as possible. Actually as observed in our previous work, the nuclear modification factor keeps unitary at the low  $p_T$  after removing the contribution from radial flow [53]. Via fitting the  $T_{kin}$  distribution by Eq. (5) the heat capacity per particle  $C_V$  was extracted.

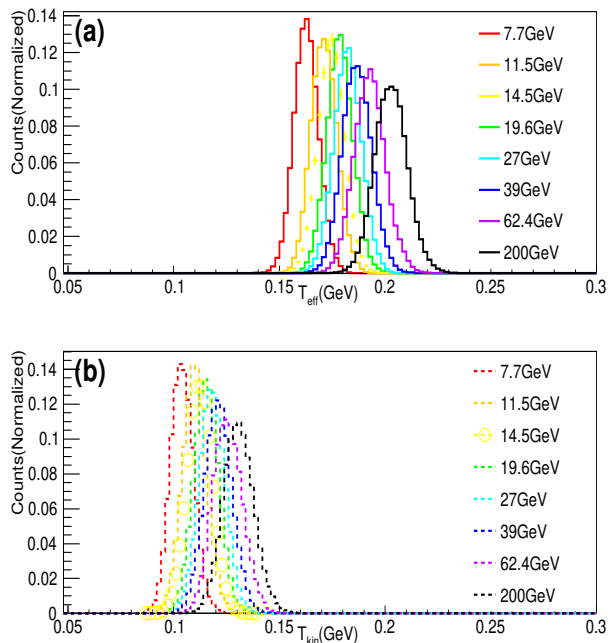


FIG. 2. The event-by-event effective temperature (a) and kinetic temperature (b) distribution at  $\sqrt{s_{NN}} = 7.7 - 200$  GeV in 0–10% central Au + Au collisions by using the String Melting AMPT.

In Fig. 3 the extracted  $C_V$  by temperature fluctua-

tion method from the STAR data decreases with the increasing of  $\sqrt{s_{NN}}$  [29]. Meanwhile the AMPT result from Ref. [29] was denoted as open square in Fig. 3, and AMPT results from our work were denoted as filled square. HRG model [29] shows the similar energy dependence of  $C_v$  and other results from HM [28], QGM [28] and so on [29] give a constant value of  $C_v$  in a wide range of  $\sqrt{s_{NN}}$ . The results present significant model dependence at low  $\sqrt{s_{NN}}$  and are consistent with each other at high  $\sqrt{s_{NN}}$  [28, 29, 34]. While when  $\sqrt{s_{NN}}$  goes down to 40 GeV and below, fluctuation of  $C_V$  dominates over the significant rising trend which may be caused by critical phase transition.

In Refs. [28, 29], the significant difference between the AMPT simulation and the enhancement structure from the data of the STAR collaboration or the HRG model [29] at low  $\sqrt{s_{NN}}$  may be related to a few points:

(1) Uncertainties of  $C_v$  are contributed by finite particle multiplicity, choice of kinetic window of  $p_T$  and fit parameters in Eq. (1), which was mentioned in Refs. [28, 29] as well;

(2) In much theoretical derivation, the system evolved in perfect thermodynamic conditions, which means the system volume is fixed and multiplicity should be high enough. However, these conditions can hardly be satisfied in real collision experiments, as noted in Ref. [28];

Two reasons mentioned above are both independent of models. Besides, the model dependence should also be commented, different model frames provide different additional uncertainty, which may be caused by different mechanism used in models, even the results are calculated in the same kinetic window of transverse momentum and rapidity.

In the following, we will try to discuss the insensitivity of temperature fluctuation in the AMPT frame partly.

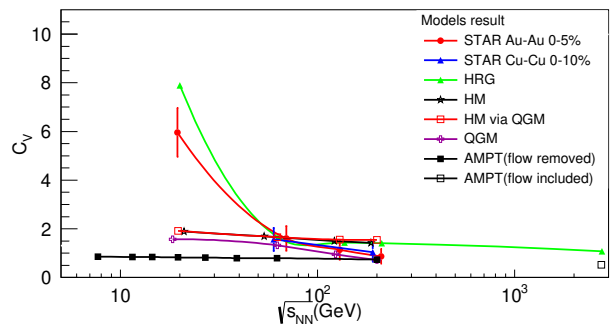


FIG. 3. The energy dependence of specific heat  $C_v = \frac{C}{N}$  extracted by different model data [29].

### III. DERIVATION OF $C_v^{\xi*}$

To avoid the model dependence of extracted specific heat, the definition of heat capacity according to Ref. [54]

can be written as

$$C = \left( \frac{\partial E_{th}}{\partial T} \right)_V, \quad (7)$$

where  $E_{th}$  is the energy of thermal motion in researched system,  $T$  is the temperature with a fixed volume of the system. Actually the definition of the heat capacity by Eq. (7) and Eq. (5) are equivalent. In Ref. [54] there is nothing different but the first one is defined from differential of enthalpy in Eq. (14.6) of Chapter 15 and the second one is derived from fluctuation in Eq. (111.6) of Chapter 12.

The definition in Eq. (7) can be combined with following assumptions :

(1)The energy of  $\pi^+$  system at final state  $- E -$  has positive correlation to  $\sqrt{s_{NN}}$ , which means for each certain collision at final state, total energy of  $\pi^+$  system evolves along a certain curve with  $\sqrt{s_{NN}}$  [55];

(2)Estimated phase volume can be approximately calculated as charged particle multiplicity  $N$ , which means we can calculate specific heat per particle  $C_v = \frac{C}{N}$  and link events to ensure enough multiplicity (here over one thousand) [28, 29];

(3)The system made up of  $\pi^+$  undergoes a hadronic interaction procedure and reaches the kinetic freeze-out stage. Then the energy contributed by hadron interaction in the system can be ignored in calculating the heat capacity.

(4)The total energy of system is mainly dominated by transverse momentum with  $\pi^+$  at mid-rapidity, which can be concluded from the transverse velocity distribution for  $\pi^+$  as shown in Fig. 4, most  $\pi^+$  distributed in the region over  $0.8c$ . So  $\pi^+$ 's energy can be written as a function of  $p_T$ . Considering the radial flow, the total energy can be written as  $E = E_{th} + E_R$  where  $E_{th}$  is internal energy from thermal motion and  $E_R$  is energy from collective radial flow [29]. In theoretical viewpoint, the heat capacity should only be contributed by  $E_{th}$ , but to avoid ambiguous differential of  $E_R$ , we firstly use total energy  $E$  to derive our effective heat capacity. The following calculation will show us that, though derived effective heat capacity includes contribution from  $E_R$ , the radial flow still can not dominate the energy dependence and fluctuation properties of heat capacity. This fact ensures our calculation and discussion on new derived heat capacity reasonable.

In Eq. (3) we gave the relation between  $T_{kin}$  and radial flow. Meanwhile the total energy of a  $\pi^+$  system can also be written as [31, 41]:

$$E = \sum_{i=1}^N E_i = \sum_{i=1}^N (p_{Ti}^2 + p_{zi}^2 + m_0^2)^{\frac{1}{2}}. \quad (8)$$

By calculating the variance and correlation coefficient of  $T_{kin}$  and radial flow, we can prove that in following derivation of  $C_v$ , the  $E_{th}$  can be replaced by total energy  $E$  in Eq. (8) reasonably.

Here we discuss the contribution from radial flow. It should note that we did not remove  $f(\langle\beta_T\rangle)$  from  $E$  directly because our  $\beta_T$  is not completely same as the one

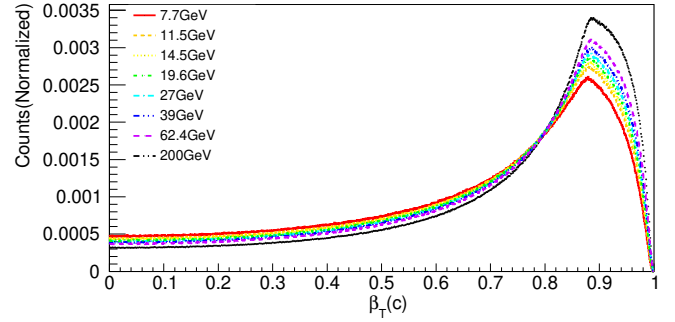


FIG. 4. The  $\beta_T$  distribution for  $\pi^+$  system at  $\sqrt{s_{NN}} = 7.7 - 200$  GeV in 0-10% central Au+Au collisions by using the String Melting AMPT model.

in the Blast-Wave Model in energy composition (though in temperature calculation our  $\beta_T$  approximately equals to  $\beta_T$  from the Blast-Wave model [50, 52]). Thus we can not simply write the energy contributed by radial flow as formation of non-relativistic kinetic energy [52, 56, 57].

In Eq. (3), the variance of  $T_{eff}$  can be written as,

$$\sigma_{T_{eff}}^2 \approx \sigma_{T_{kin}}^2 + m_0^2 \sigma_{\langle\beta_T\rangle^2} + 2m_0 \text{Cov}(T_{kin}, \langle\beta_T\rangle^2). \quad (9)$$

Fig. 5 shows the variance of  $T_{eff}$  and each term in the right side of Eq. (9). It can be seen that the variance from  $T_{kin}$  dominates the one for  $T_{eff}$  while the one from  $\langle\beta_T\rangle^2$  is less with one order of magnitude, thus the statistical properties of  $\langle\beta_T\rangle$  can be negligible in properties of temperature.

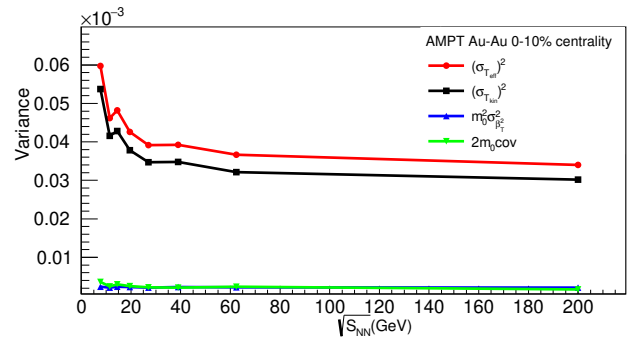


FIG. 5. The variance of each term in temperature from the String Melting AMPT model.

Then in Fig. 6 we calculated the linear correlation coefficient  $\eta = \text{Cov}(T_{kin}, \langle\beta_T\rangle^2) / (\sigma_{T_{kin}} \sigma_{\langle\beta_T\rangle^2})$ , here  $\eta \leq 0.2$  means that they are linear independent, in addition the differential relation of  $T_{kin}$  and  $T_{eff}$  is approximately a constant, thus when discussing differential relation, we can use  $T_{eff}$  instead of  $T_{kin}$  for differential term from radial flow.

Based on the assumptions above, the energy dependence of  $C_v$  for  $\pi^+$  system can be described as following figure: At different  $\sqrt{s_{NN}}$ , each  $\pi^+$  system can be seen to evolve along one unique path. The continuous changing

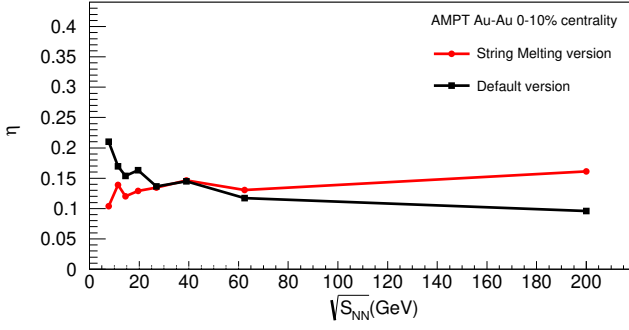


FIG. 6. The correlation coefficient between  $T_{kin}$  and  $\beta_T^2$  in different versions.

kinetic parameters make sure that when  $\sqrt{s_{NN}}$  changes, the total energy  $E$  of  $\pi^+$  system changes to  $E + \Delta E$ , the  $p_T$  spectrum changes, resulting  $p_T$  of each  $\pi^+$  changes to  $p_T + \Delta p_T$ . The linked events ensured similar multiplicity when  $E$  changes, thus for each  $\pi^+$  we can find a closest new  $\pi^+$  in phase space with  $p_T + \Delta p_T$ . In this sense,  $E$  and  $p_T$  for each  $\pi^+$  can be seen as functions of system temperature.

From Eq. (7) and Eq. (8), we get

$$\begin{aligned}
 \frac{\partial E}{\partial T}|_{E(T)} &= \sum_i^N \frac{\partial}{\partial T} (p_{Ti}^2 + p_{zi}^2 + m_0^2)^{\frac{1}{2}} \\
 &= \sum_i^N \frac{\partial E_i}{\partial p_{Ti}} \frac{\partial p_{Ti}}{\partial T} \\
 &= \sum_i^N \frac{1}{2} \frac{2p_{Ti}}{E_i} \frac{\partial p_{Ti}}{\partial T} \\
 &= \sum_i^N \left( \beta_{Ti} \frac{\partial p_{Ti}}{\partial T} \right) |_{E(T)}.
 \end{aligned} \tag{10}$$

The sum can be converted to the integral pattern with help of Riemann Sum. Let  $f(x_i) = F(x_i)/\Delta x_i$ , for equidistant division, the Riemann integral can be written as

$$\int_a^b f(x) g(x) dx \approx \sum_i^{(b-a)/\Delta x} \frac{F(x_i)}{\Delta x} g(x_i) \Delta x. \tag{11}$$

It should be noted here  $N_x$  stands for the number of division in Riemann integral which is different from multiplicity  $N_{multi}$ , but we can approximately let  $(b-a)/\Delta x = N_x = N_{multi}$ , so that the definition of  $C_v$  expressed by sum can relate to integral over temperature, in the integral  $(a, b)$  means integral range. As mentioned in Ref. [28] and Ref. [29], linked events ensured enough multiplicity and small error for fitting.

Now we got

$$\begin{aligned}
 \sum_i^{N_{multi}} \beta_{Ti} \frac{\partial p_{Ti}}{\partial T} |_T &= \sum_i^{(b-a)/\Delta x} \frac{\beta_{Ti}}{\Delta T} \frac{\partial p_{Ti}}{\partial T} \Delta T \\
 &\approx \int_a^b \frac{\beta_{Ti}}{dT} \frac{\partial p_{Ti}}{\partial T} dT \\
 &= \left( \frac{\beta_{Ti}}{dT} \frac{\partial p_{Ti}}{\partial T} \right) \Big|_{T=\xi} (b-a) \tag{12} \\
 &\approx \tilde{\beta}_T \frac{\partial \tilde{p}_T}{\partial T} \Big|_{T=\xi} \frac{(b-a)}{\Delta T} \\
 &= N_{multi} \left( \tilde{\beta}_T \frac{\partial \tilde{p}_T}{\partial T} \right) \Big|_{T=\xi}.
 \end{aligned}$$

In Mean Value Theorem of Integrals  $\tilde{\beta}_T$  and  $\tilde{p}_T$  are points proved to exist to reveal the property of dependence for  $E$  and  $T$ . Hence the derivation gave the specific heat expressed by kinetic quantities

$$C_v^\xi = \frac{C}{N_{multi}} \approx \tilde{\beta}_T(\xi) \frac{\partial \tilde{p}_T}{\partial T} \Big|_\xi. \tag{13}$$

In Eq. (13) and Eq. (10), the heat capacity for ensemble can be expressed as a combination of kinetic measurements in a characteristic event whose  $T = \xi$ .

The work gave a specific heat approximately expressed by transverse velocity, transverse momentum and temperature in a unique event ' $\xi$ ' and derivative of transverse momentum to temperature in a unique event ' $\xi$ '. We should note here, it seems that  $C_v^{\xi*}$  includes radial flow term by  $\beta_T$ , but according to Ref. [50], at low  $\sqrt{s_{NN}}$   $\beta_T$  decreases and  $f(\langle \beta_T \rangle)$  is smaller than  $T_{kin}$ , the dominant contribution is actually from thermal motion. That is why in Eq. (7) we can use  $E$  instead of  $E_{th}$ . Since the first mean value theorem for integrals can only provide the existence of ' $\xi$ ', it can not find the accurate event to calculate the  $C_v^\xi$ , so the study further used mean value of kinetic quantities instead of unique one to give accessible results that can be measured and computed from data:

$$C_v^{\xi*} = \overline{\beta_T} \frac{\partial \overline{p_T}}{\partial T} \Big|_{T=T_{eff}}. \tag{14}$$

In Eq. (14), according to Eq. (7)'s definition, we should use  $T_{kin}$  as  $T$  in calculation of  $\overline{p_T}$ , but this formation involving radial flow can not give identical formation of  $\frac{\partial \overline{p_T}}{\partial T_{kin}}$ , fortunately in Fig. 5 and Fig. 6 it can be calculated by the AMPT result that differential for  $T_{kin}$  and  $T_{eff}$  has strongly linear dependence, we can directly use  $T_{eff}$  instead of  $T_{kin}$  in  $\frac{\partial \overline{p_T}}{\partial T}$ . Now we can conveniently calculate  $\frac{\partial \overline{p_T}}{\partial T} |_{T=T_{eff}}$  based on the  $p_T$  spectrum [50, 58–60]:

$$\begin{aligned}
 \overline{p_T} &= \frac{\int_{p_{min}}^{p_{max}} p_T^2 F(p_T) dp_T}{\int_{p_{min}}^{p_{max}} p_T F(p_T) dp_T} \\
 &= 2T_{eff} \\
 &+ \frac{p_{min}^2 e^{-p_{min}/T_{eff}} - p_{max}^2 e^{-p_{max}/T_{eff}}}{(p_{min} + T_{eff}) e^{-p_{min}/T_{eff}} - (p_{max} + T_{eff}) e^{-p_{max}/T_{eff}}}.
 \end{aligned} \tag{15}$$

Considering the mean value and unique value are obviously different, which directly connected to our explanation on the statistical parameters, we will discuss the topic in the next section.

#### IV. RESULTS AND DISCUSSION

According to the derived formula (14) and (15),  $C_v^{\xi*}$  is calculated with data of  $\pi^+$  system in Au + Au collisions at different  $\sqrt{s_{NN}}$  simulated by AMPT and the event-by-event distribution of  $C_v^{\xi*}$  presents the Gaussian distribution as shown in Fig. 7. From the event by event distribution, a mean value of  $C_v^{\xi*}$  at each  $\sqrt{s_{NN}}$  is obtained, denoted as  $\langle C_v^{\xi*} \rangle$ .

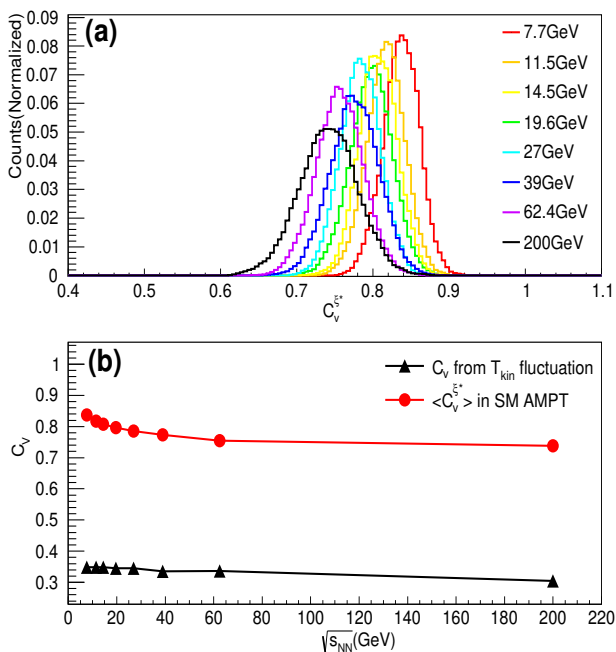


FIG. 7. (a) The  $C_v^{\xi*}$  event-by-event distribution for  $\pi^+$  system in 0 – 10% central Au+Au collisions,  $\sqrt{s_{NN}} = 7.7, 11.5, 14.5, 19.6, 27, 39, 62.4,$  and 200 GeV by using the String Melting AMPT; (b) The extracted  $\langle C_v^{\xi*} \rangle$  from the String Melting AMPT model calculation in red line, compared to the  $C_v$  from  $T_{kin}$  fluctuation which is represented by the black line.

In Figure 7(b)  $\langle C_v^{\xi*} \rangle$  from the AMPT calculations showed a decreasing trend with the increasing of  $\sqrt{s_{NN}}$ . Compared to the results in Ref. [28], the energy dependence of  $\langle C_v^{\xi*} \rangle$  is similar to the results of QGM and HM via QGM in Fig. 3, showing a rising trend as  $\sqrt{s_{NN}}$  decreases (though the value of  $C_V$  and  $\langle C_v^{\xi*} \rangle$  are slightly different), meanwhile the result of HM showed an inflection point at low  $\sqrt{s_{NN}}$ . In Ref. [28]’s explanation, the big difference of specific heat between QGM, pQCD thermodynamic method (with a peak structure,  $C_V \sim 10$ ) and approximate pure gauge theory (with a peak struc-

ture,  $C_V \sim 15$ ) should be studied further to confirm the discrepancy contributed by classical and quantum statistics. So they suggested using RHIC single event charged  $\pi^+$  system  $p_T$  distribution to extract  $C_V$  according to statistical method same as Ref. [28]. For our calculation of  $C_v^{\xi*}$ , we suggest extracting transverse velocity and effective temperature from  $p_T$  spectrum. Considering the difficulty in particle identification and measurement, an alternative method to extract these parameters is fitting by the Blast-Wave model as the method in Ref. [50]. Since the original definition for  $\beta_T$  and  $T_{kin}$  according to Ref. [50] showed slight difference to that in this work, both of them give the same physical description of the evolution properties for the fireball. So the suggested method to extract parameters for  $C_v^{\xi*}$  desires smaller uncertainty, clear energy dependence, and spectrum for linked events of charged  $\pi$  system in practical for experiments.

To clearly illustrate the sensitivity of  $C_v^{\xi*}$  to  $\beta_T$  and  $T_{kin}$ , we plot  $C_v^{\xi*}$  as functions of  $\beta_T$  and  $T_{kin}$  in Fig.8. An inflection point exists at around  $T_{eff} = 100$  MeV, which depends on the fitting limits of  $p_T$  spectrum. The combination of linear dependence of  $\beta_T$  and non-monotonic dependence of  $T_{eff}$  results in that  $C_v^{\xi*}$  is sensitive to the range of the fitting parameters by the blast-wave model. Along an identified curve of  $C_v^{\xi*}$  in Fig. 8, a shifting fitting result may cause different trend of  $C_v^{\xi*}$  energy dependence, which has to be studied further, especially near the QCD critical point.

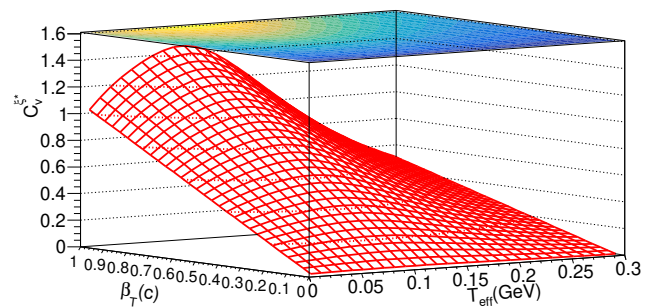


FIG. 8. The theoretical  $C_v^{\xi*}$  distribution as a two-dimensional function of  $\beta_T$  and  $T_{eff}$ .

In Fig. 7(b) the mean values of  $C_v^{\xi*}$  are smaller than those extracted from HRG model, HM model, QGM model [28]. In the first mean value theorem for integrals, mean value deviates the ideal  $C_v^{\xi}$ . That means only if one can accurately find the evolution curve of a characteristic event corresponding to temperature  $\xi$ , the real  $C_v^{\xi}$  can agree with results extracted by temperature fluctuation from the STAR’s data especially at low  $\sqrt{s_{NN}}$  [29]. It is interesting to see that  $\langle C_v^{\xi*} \rangle$  remained the rising trend at low  $\sqrt{s_{NN}}$ , which suggested that in the event-by-event distribution we can still find special properties similar to the peak structure [42].

As a measurement of heat capacity, the behaviour of

$C_v^{\xi*}$  with parton process or only with hadron process are different. Though the rising trend of average  $C_v^{\xi*}$  is depressed, the events with parton process can provide higher  $C_v^{\xi*}$  similar to pQCD and other models [28, 29]. That means more events with higher  $C_v^{\xi*}$  emerge at low  $\sqrt{s_{NN}}$ . Further, both  $C_v^{\xi}$  and  $T$  distribution are used to measure fluctuation, so we can investigate the fluctuation behaviour as we did in temperature distribution. It means rising trend with smaller variance can be shown as a narrow peak of both temperature and  $C_v^{\xi*}$  distribution.

Based on the event by event distribution of  $C_v^{\xi*}$ , skewness and kurtosis of  $C_v^{\xi*}$  can be obtained in the AMPT model with the String Melting and Default version, respectively. The skewness and kurtosis are defined as  $\frac{\mu_3}{\sigma^3}$  and  $\frac{\mu_4}{\sigma^4} - 3$ , respectively. Here  $\mu_n = \langle (X - \langle X \rangle)^n \rangle$  and  $\sigma = \sqrt{\frac{\sum (X_i - \langle X \rangle)^2}{N}}$  where the  $X$  represents  $C_v^{\xi*}$ . The skewness reflects the deviation of  $C_v^{\xi*}$  distribution from Gaussian distribution, and the kurtosis describes how close the events distribute to expectancy (a standard Gaussian distribution has zero kurtosis). At RHIC, skewness and kurtosis has been successfully applied to net-proton fluctuation to explore possible QCD critical point [4, 61–64]. Here we use this kind of high-order moment to specific heat analysis. Fig. 9(a) and (b), respectively, showed the skewness and kurtosis as a function of  $\sqrt{s_{NN}}$ . We can find that they were indeed obviously different at low  $\sqrt{s_{NN}}$ . In the String Melting version, at low  $\sqrt{s_{NN}}$  the skewness and kurtosis all showed a sharp enhanced structure around 20 GeV or lower  $\sqrt{s_{NN}}$ . Meanwhile in the Default version, the skewness and kurtosis are both close to zero and present independence on  $\sqrt{s_{NN}}$ .

Before discussing the statistical properties obtained from  $C_v^{\xi*}$ , we need to discuss statistical fluctuation. According to Ref. [29], the contribution of statistical fluctuation in  $T_{eff}$  distribution can be written as  $(\Delta T_{eff})^2 = (\Delta T_{eff}^{dyn})^2 + (\Delta T_{eff}^{sta})^2$ . In Ref. [29], they extracted the statistical fluctuation by randomly mixed data from experiments, and then removed the width of the randomly mixed temperature distribution. We randomly mixed the data from the AMPT calculation while making sure the multiplicity in each event is close to the one in our linked events at about 1000, then we extracted skewness and kurtosis of the randomly mixed  $C_v^{\xi*}$  distribution to compare with the results from two versions of AMPT.

In Figure 9(a) and (b), we can clearly find the results from the randomly mixed events and the Default version AMPT are close to each other, which means the energy dependence of skewness and kurtosis in the Default version without partonic process are mainly contributed by statistical fluctuation. Meanwhile, at low  $\sqrt{s_{NN}}$  the String Melting version showed clearly an enhancement structure far from both the Default version and random mixed one. This comparison indicated the unique behavior of 3rd and 4th order moment from the String Melting version at low  $\sqrt{s_{NN}}$  are mainly from the dynamical fluctuation, which reflected that the special properties of

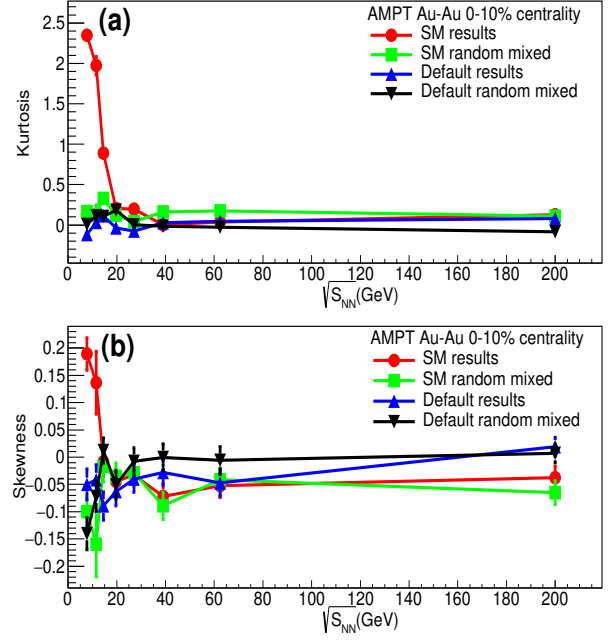


FIG. 9. The energy dependence of kurtosis (a) and skewness (b) of  $C_v^{\xi*}$  for  $\pi^+$  system from the String Melting AMPT in red line, compared to the green line (Default version), blue and black line (random mixed statistical fluctuation).

thermodynamic quantities indeed survived partonic and hadronization process – even partly. Besides we can also compare the Default result and the random mixed one, and see only slight difference. Though negligible to the enhancement structure in the String Melting version, we can still see, the self-correlation of linked events can significantly suppress kurtosis and skewness at low  $\sqrt{s_{NN}}$ .

The difference between two versions, namely with or without partonic interaction process, shows different thermal properties. When  $\sqrt{s_{NN}}$  decreases, skewness of  $C_v^{\xi*}$  from the String Melting version increases rapidly to a high positive value. That means, compared to the default version, more events with higher  $C_v^{\xi*}$  distributed on the right side of mean value. As mentioned in this section, the real  $C_v^{\xi}$  obtained from ' $\xi$ ' was depressed by average over the events, but the positive skewness indicated that parton phase in the String Melting version contributes higher value of  $C_v^{\xi}$  than that in the Default AMPT version. The higher value indicates that, in the String Melting version of AMPT, the heat capacity of  $\pi^+$  system behaves more similarly to prediction in other models or theories [28, 29] than the Default version. Here it is explained the positive skewness as a signal for formation of  $\pi^+$  system close to the real  $C_v^{\xi}$  state, instead of explained as overall enhancement of  $\pi^+$  system state, because if so, one should find the event-by-event distribution moved totally into a higher range and still followed the standard Gaussian distribution.

As for the String Melting version, our kurtosis for

$C_v^{\xi*}$  distribution is close to zero at high  $\sqrt{s_{NN}}$  and rose rapidly to highly positive values around 20 GeV or lower. Meanwhile we can see the kurtosis from the Default version keeps close to zero both at high and low  $\sqrt{s_{NN}}$ . The low kurtosis in the Default version indicates that if we choose AMPT with hadron gas phase instead of parton phase, the  $C_v^{\xi*}$  distribution shows similarity to the standard Gaussian distribution. The sharp enhancement in the SM version shows that the  $\pi^+$  system formed after parton phase drives events to a distribution with much lower  $\sigma$  than the one formed from hadron gas. Comparing to Eq. (5) it can be found that though  $\sigma$  for  $C_v^{\xi*}$  and  $T_{kin}$  or  $T_{eff}$  are different, they both reflect the significant change of system event-by-event fluctuation. As in results from other models or data the enhancement structure of  $C_v$  at low  $\sqrt{s_{NN}}$  shows the fluctuation of temperature extends to system size of all events in ensemble, the enhancement structure of  $C_v^{\xi*}$ 's kurtosis shows the fluctuation of  $C_v^{\xi*}$  behaves similarly [7, 8, 12], which indicates the unique properties of charged particles formed via parton phase are significantly different from those experienced no partonic process. Hence the energy dependence of  $C_v^{\xi*}$  with skewness and kurtosis could be alternative, significant and verifiable signal to investigate the nature around the critical point of hot dense matter created in heavy-ion collisions.

## V. SUMMARY

In this work, we studied the energy dependence of specific heat in a framework of AMPT model. Our work obtained specific heat by event-by-event fluctuation for  $\pi^+$  system from the AMPT and compared the results with those from the STAR's data [29] and other models [28], then analyzed their difference and the potential reasons. Based on a few assumptions, we derived a new form, namely  $C_v^{\xi*}$ , from characteristic event's kinetic quantities to describe specific heat. By using AMPT model

[31, 38, 41], this work presents the  $\sqrt{s_{NN}}$  dependence of  $C_v^{\xi*}$  and the skewness and kurtosis for event-by-event distribution of  $C_v^{\xi*}$ . Our work found the  $C_v^{\xi*}$  behaved closer to results from the HRG and STAR's data than  $C_v$  from temperature fluctuation in the AMPT frame but still too small to reflect the enhancement structure at low  $\sqrt{s_{NN}}$  because of the depression of average and effect of radial flow. So it further gave the event-by-event distribution of  $C_v^{\xi*}$  and the obtained expectancy, skewness and kurtosis of the distribution. To ensure the calculation reasonable, it additionally compared the variance of different terms and linear correlation coefficient. We compared parameters like skewness and kurtosis in two different versions of AMPT. According to skewness we found the String Melting version with parton phase showed clearer properties of  $\pi^+$  system than the Default version. More  $\pi^+$  events at higher specific heat state emerge after a partonic process. And from kurtosis it can be seen that the behavior of fluctuation of  $C_v^{\xi*}$  in the String Melting version is similar to the behavior of fluctuation of temperature described by  $C_v$  from results of Refs. [10, 28, 29, 34]. So in future, we expected more experimental and theoretical investigation using the heat capacity to search for the QCD phase transition of the hot dense matter created in heavy-ion collisions.

## ACKNOWLEDGMENTS

This work was supported in part by the National Natural Science Foundation of China under contract Nos. 11890710, 11890714, 11875066, 11925502, 11961141003 and 12147101, the Strategic Priority Research Program of CAS under Grant No. XDB34000000, National Key R&D Program of China under Grant No. 2016YFE0100900 and 2018YFE0104600, and by Guangdong Major Project of Basic and Applied Basic Research No. 2020B0301030008.

- 
- [1] A. Bzdak, S. Esumi, V. Koch, J. Liao, M. Stephanov, and N. Xu, *Phys. Rep.* **853**, 1 (2020).
  - [2] E. Shuryak, *Rev. Mod. Phys.* **89**, 035001 (2017).
  - [3] P. Braun-Munzinger, V. Koch, T. Schäfer, and J. Stachel, *Phys. Rep.* **621**, 76 (2016).
  - [4] X. F. Luo and N. Xu, *Nucl. Sci. Tech.* **28**, 112 (2017).
  - [5] S. Wu, C. Shen, and H. Song, *Chin. Phys. Lett.* **38**, 081201 (2021).
  - [6] M. Waqas, F.-H. Liu, L.-L. Li, and H. M. Alfanda, *Nucl. Sci. Tech.* **31**, 109 (2020).
  - [7] A. Puglisi, A. Sarracino, and A. Vulpiani, *Phys. Rep.* **709-710**, 1 (2017).
  - [8] A. Ayala, M. Hentschinski, L. Hernández, M. Loewe, and R. Zamora, *Ukr. J. Phys.* **64**, 665 (2019).
  - [9] A. Ayala, M. Hentschinski, L. A. Hernández, M. Loewe, and R. Zamora, *Phys. Rev. D* **98**, 114002 (2018).
  - [10] S. Basu, R. Chatterjee, B. K. Nandi, and T. K. Nayak, (2015), [arXiv:1504.04502](https://arxiv.org/abs/1504.04502) [nucl-ex].
  - [11] E. V. Shuryak, *Phys. Lett. B* **423**, 9 (1998).
  - [12] L. Stodolsky, *Phys. Rev. Lett.* **75**, 1044 (1995).
  - [13] Z. Han, B. Chen, and Y. Liu, *Chin. Phys. Lett.* **37**, 112501 (2020).
  - [14] J. C. Pan, S. D. Gupta, and M. Grant, *Phys. Rev. Lett.* **80**, 1182 (1998).
  - [15] G. G. Chaudhuri and S. D. Gupta, *Phys. Rev. C* **76**, 014619 (2007).
  - [16] Y. G. Ma, *Phys. Rev. Lett.* **83**, 3617 (1999).
  - [17] M. D'Agostino, F. Gulminelli, P. Chomaz, *et al.*, *Phys. Lett. B* **473**, 219 (2000).
  - [18] J. B. Natowitz, K. Hagel, Y. G. Ma, *et al.*, *Phys. Rev. Lett.* **89**, 212701 (2002).
  - [19] F. Gulminelli, P. Chomaz, A. H. Raduta, and A. R.



- Raduta, *Phys. Rev. Lett.* **91**, 202701.
- [20] Y. G. Ma, J. B. Natowitz, R. Wada, *et al.*, *Phys. Rev. C* **71**, 054606 (2005).
- [21] C. W. Ma and Y.-G. Ma, *Prog. Part. Nucl. Phys.* **99**, 120 (2018).
- [22] W. Lin, P. Ren, and R. Wada, *Phys. Rev. C* **99**, 054616 (2019).
- [23] B. Borderie and J. Frankland, *Prog. Part. Nucl. Phys.* **105**, 82 (2019).
- [24] H. L. Liu, Y. G. Ma, and D. Q. Fang, *Phys. Rev. C* **99**, 054614 (2019).
- [25] G. L. Ma, Y. G. Ma, B. H. Sa, *et al.*, *HIGH ENERG PHYS NUC* **28**, 398 (2004).
- [26] Y. G. Ma, G. L. Ma, X. Z. Cai, *et al.*, *J. Phys. G* **31**, S1179 (2005).
- [27] X. H. Shi, G. L. Ma, Y. G. Ma, X. Z. Cai, and J. H. Chen, *Int. J. Mod. Phys. E* **16**, 1912 (2007).
- [28] B.-H. Sa, X.-M. Li, S.-Y. Hu, S.-P. Li, J. Feng, and D.-M. Zhou, *Phys. Rev. C* **75**, 054912 (2007).
- [29] S. Basu, S. Chatterjee, R. Chatterjee, T. K. Nayak, and B. K. Nandi, *Phys. Rev. C* **94**, 044901 (2016).
- [30] S. Jeon and V. Koch, “Event by event fluctuations,” in *Quark-gluon plasma. Vol. 3*, edited by R. Hwa and X. Wang (2004) pp. 430–490, [arXiv:hep-ph/0304012](https://arxiv.org/abs/hep-ph/0304012).
- [31] Z.-W. Lin, C. M. Ko, B.-A. Li, B. Zhang, and S. Pal, *Phys. Rev. C* **72**, 064901 (2005).
- [32] G.-L. Ma and Z.-W. Lin, *Phys. Rev. C* **93**, 054911 (2016).
- [33] Z.-W. Lin and L. Zheng, *Nucl. Sci. Tech.* **32**, 113 (2021).
- [34] S. Deb, G. Sarwar, R. Sahoo, and J.-e. Alam, *Eur. Phys. J. A* **57**, 195 (2021).
- [35] X.-N. Wang and M. Gyulassy, *Phys. Rev. D* **44**, 3501 (1991).
- [36] M. Gyulassy and X.-N. Wang, *Comp. Phys. Comm.* **83**, 307 (1994).
- [37] B. Zhang, *Comp. Phys. Comm.* **109**, 193 (1998).
- [38] B.-A. Li and C. M. Ko, *Phys. Rev. C* **52**, 2037 (1995).
- [39] X.-H. Jin, J.-H. Chen, Y.-G. Ma, *et al.*, *Nucl. Sci. Tech.* **29**, 54 (2018).
- [40] H. Wang, J. H. Chen, Y. G. Ma, *et al.*, *Nucl. Sci. Tech.* **30**, 185 (2019).
- [41] Z.-W. Lin, *Phys. Rev. C* **90**, 014904 (2014).
- [42] M. Mukherjee, S. Basu, A. Chatterjee, S. Chatterjee, S. P. Adhya, S. Thakur, and T. K. Nayak, *Phys. Lett. B* **784**, 1 (2018).
- [43] C. Shen and Y. Li, *Nucl. Sci. Tech.* **31**, 122 (2020).
- [44] X.-L. Zhao, G.-L. Ma, and Y.-G. Ma, *Phys. Rev. C* **99**, 034903 (2019).
- [45] J.-H. Gao, G.-L. Ma, S. Pu, and Q. Wang, *Nucl. Sci. Tech.* **31**, 90 (2020).
- [46] Y.-C. Liu and X.-G. Huang, *Nucl. Sci. Tech.* **31**, 56 (2020).
- [47] C.-Z. Wang, W.-Y. Wu, Q.-Y. Shou, G.-L. Ma, Y.-G. Ma, and S. Zhang, *Phys. Lett. B* **820**, 136580 (2021).
- [48] X. L. Zhao, G. L. Ma, and Y. G. Ma, *Phys. Lett. B* **792**, 413 (2019).
- [49] W.-Y. Wu, C.-Z. Wang, Q.-Y. Shou, Y.-G. Ma, and L. Zheng, *Phys. Rev. C* **103**, 034906 (2021).
- [50] L. Adamczyk *et al.* (STAR Collaboration), *Phys. Rev. C* **96**, 044904 (2017).
- [51] M. Waqas, F.-H. Liu, and Z. Wazir, *Adv. High Energy Phys.* **2020**, 8198126 (2020).
- [52] F. Retière and M. A. Lisa, *Phys. Rev. C* **70**, 044907 (2004).
- [53] M. Lv, Y. G. Ma, G. Q. Zhang, J. H. Chen, and D. Q. Fang, *Phys. Lett. B* **733**, 105 (2014).
- [54] L. D. Landau and E. M. Lifshitz, *Course of Theoretical Physics* (1980).
- [55] J. Adams *et al.* (STAR Collaboration), *Phys. Rev. C* **70**, 054907 (2004).
- [56] B. I. Abelev *et al.* (STAR Collaboration), *Phys. Rev. C* **79**, 034909 (2009).
- [57] J. Adam *et al.* (ALICE Collaboration), *Phys. Rev. C* **93**, 024917 (2016).
- [58] J. Adams *et al.*, *Nucl. Phys. A* **757**, 102 (2005), first Three Years of Operation of RHIC.
- [59] F. G. Gardim, G. Giacalone, M. Luzum, and J.-Y. Ollitrault, *Nature Phys.* **16**, 615 (2020).
- [60] L. Adamczyk *et al.* (STAR Collaboration), *Phys. Rev. C* **87**, 064902 (2013).
- [61] M. A. Stephanov, *Phys. Rev. Lett.* **107**, 052301 (2011).
- [62] M. M. Aggarwal *et al.* (STAR Collaboration), *Phys. Rev. Lett.* **105**, 022302 (2010).
- [63] L. Adamczyk *et al.* (STAR Collaboration), *Phys. Rev. Lett.* **112**, 032302 (2014).
- [64] J. Adam *et al.* (STAR Collaboration), *Phys. Rev. Lett.* **126**, 092301 (2011).